The solution structure of 1:2 phenol/N-methylpyridinium bis{(trifluoromethyl)sulfonyl}imide liquid mixtures

Turner, A. H., & Holbrey, J. D. (2015). The solution structure of 1:2 phenol/N-methylpyridinium bis{(trifluoromethyl)sulfonyl}imide liquid mixtures. *Journal of Solution Chemistry*, *44*(3-4), 621-633. https://doi.org/10.1007/s10953-015-0296-2

Published in:
Journal of Solution Chemistry

Document Version:
Peer reviewed version

Journal of Solution Chemistry manuscript No.
(will be inserted by the editor)

The solution structure of 1:2 phenol/*N*-methylpyridinium *bis*{(trifluoromethyl)sulfonyl}imide liquid mixtures

Adam H. Turner · **John D. Holbrey**

Received: date / Accepted: date

Abstract Neutron diffraction has been used to investigate the liquid structure of a 1:2 solution of phenol in the ionic liquid *N*-methylpyridinium *bis*{(trifluoromethyl)-sulfonyl}imide at 60 °C, using the empirical potential structure refinement (EPSR) process to model the data obtained from the SANDALS diffractometer at ISIS. Addition of phenol results in suppression of the melting point of the pyridinium salt and formation of a room temperature solution with aromatic phenol–cation and phenol-OH to anion hydrogen-bonding interactions.

Keywords Ionic Liquids · Phenol · Deep Eutectic Solvents · Neutron Scattering · Liquid Structure · Extraction

1 Introduction

Phenols are widely used as intermediates for plastics, polymers, drugs such as aspirin, dyes, pesticides, wood preservatives, *etc* [1]. However, as well as being important industrial chemicals, they are also of concern with regard to health and environmental contamination. The US Environmental Protection Agency labels phenols as toxic, priority pollutants [2] due in part to their toxicity at low concentrations. Many phenolic compounds, including alkylphenol, pentachlorophenol, and bisphenol A are endocrine-disruptors that are hazardous to human reproductive health and present a serious source of pollution and contamination of water. EU limits for the maximum level of phenol in drinking water is 0.5 μg L^{-1} (EU Council Directive 98/83/EC on the quality of water intended for human consumption). Phenol contamination leading to environmental pollution can be caused indirectly from fuel processing activities [3]

J. D. Holbrey
School of Chemistry and Chemical Engineering,
Queen's University Belfast,
Belfast BT9 5AG, Northern Ireland, UK.
E-mail: j.holbrey@qub.ac.uk

or from the direct production of phenolic compounds by oxidation of cumene[4, 5], liquefaction of coal tars or pyrolysis of biomass [1].

Many approaches to control the release of phenols, or to address contamination are used. These include biodegradation, chemical oxidation, adsorption, membrane separation, and solvent extraction approaches [6]. Solvent extraction of phenols from water typically makes use of toxic, volatile, and flammable organic solvents (including hexane, tributyl phosphate, n-butyl acetate, diisopropyl ether, and methyl isobutyl ketone) [7].

Ionic liquids [8, 9] have been investigated as alternatives to volatile organic solvents for extraction processes. Huddleston *et al.* [10, 11] demonstrated that the partitioning of organic solutes from water to hydrophobic ionic liquids followed the solutes' octanol/water log*P* values and that changes to the aqueous phase pH could be used to strip and recover ionisable solutes. Phenols can be partitioned from water to hydrophobic ionic liquids [12–16] and used for analytical microphase extraction and preconcentration [17–21], and to produce liquid membranes to enable extraction and stripping [22, 23]. High levels of phenol extraction in a single step under acid conditions have been reported, with stripping from the ionic liquid at high pH, following the overall scheme:

$$C_5H_5OH_{(aq)} + IL \underset{OH^-}{\overset{H^+}{\rightleftharpoons}} H_2O + C_5H_5OH_{(IL)}$$

Partitioning can be enhanced by increasing the lipophilicity of the ionic liquid, for example, by increasing the size of alkyl-substituents on the cation [17]. Computational studies [24, 25] have also highlighted the importance of hydrogen bonding to the extraction mechanism. In an alternative approach to isolate phenols from coal liquefaction/gasification streams, Wu, Marsh and co-workers [26, 27] used the formation of deep eutectic solvents (DES) [28] between solid choline chloride and hydrogen-bond donors such as phenol [29] as a strategy to enable phenol separation and recovery from phenol/oil mixtures as an oil-immiscible phase without using aqueous alkali and acid.

The utility of ionic liquids, and DES systems , to remove phenols from both water and oils depends on the interactions between the solutes and ionic liquid components. Thus the ability to design ionic liquids with enhanced performance requires an understanding of the individual molecular interactions. Amongst the many methods available to investigate ionic liquids at the molecular level [30], neutron diffraction combined with computer simulation has proven a powerful tool that can reveal both the structure of pure ionic liquids [31–33], solvent-solute interactions [34–37] including the formation of π–cation aggregates in aromatic charge-transfer solutions [38], differences in amine and alcohol solvation [39], and anion interactions with glucose [40, 41] which aid understanding of the mechanisms for cellulose dissolution in ionic liquids [42, 43].

Here, we report on the the liquid structure and solvation environment of phenol dissolved at high concentration (34 mol %) in the ionic liquid, *N*-methylpyridinium *bis*{(trifluoromethyl)sulfonyl}imide ($[CH_3-Py][NTf_2]$), as determined using Empirical Potential Structure Refinement (EPSR) analysis of experimental liquid neutron diffraction data collected from H/D-isotopically substituted mixtures.

2 Experimental

2.1 Synthesis

Deuterated dimethylsulfate-d_6 was obtained from CDN Isotopes, pyridine-d_5, phenol-d_6 and all other reagents were purchased from SigmaAldrich and used as received without further purification. All the deuteriated materials had isotopic substitution greater than 98%. *N*-methylpyridinium *bis*{(trifluoromethyl)sulfonyl}imide salts with deuterium substitution at the methyl-, ring-, and methyl+ring positions respectively were synthesised by alkylation of either pyridine or deuterated pyridine with dimethylsulfate [44] (using the appropriate protiated or deuteriated isotopologues) followed by anion metathesis with lithium *bis*{(trifluoromethyl)sulfonyl}imide (Li[NTf_2]) in D_2O (ring deuteriated salts) or H_2O (ring protiated salts). In each case, the salts were obtained as hydrophobic colourless low melting crystalline solids. A representative synthesis is described below.

2.1.1 N-Methylpyridinium methylsulfate

Under an inert N_2 atmosphere, dimethyl sulfate (10 g, 81 mmol) was added dropwise *via* a syringe to pyridine (6.1 g, 77 mmol) in a round-bottomed flask heated to 50 °C. with rapid stirring. The addition rate was controlled to prevent the reaction exotherm rising above *ca.* 70 °C. After allowing the reaction mixture to cool to room temperature, the product was used directly for metathesis.

2.1.2 N-Methylpyridinium bis{(trifluoromethyl)sulfonyl}imide

Aqueous solutions of Li[NTf_2] (21.5 g, 75 mmol) and *N*-methylpyridinium methylsulfate (*ca.* 15.3 g, 71 mmol) in 35 cm^3 H_2O were combined. *N*-Methylpyridinium *bis*{(trifluoromethyl)sulfonyl}imide was immediately formed, initially as a dense colourless hydrophobic liquid that crystallised on standing at room temperature and was collected by filtration, drying in air and then *in vacuo*. Mp 43.0±0.5 °C (*lit.* [45] 43.8 °C); ^{1}H NMR (DMSO-d_6, 400 MHz): d = 4.33 (s, 3H), 8.11 (t, *J* = 7.2 Hz, 2H), 8.56 (t, *J* = 7.5 Hz, 1H), 8.97 (d, *J* = 6.0 Hz, 2H).

2.1.3 Phenol:N-Methylpyridinium bis{(trifluoromethyl)sulfonyl}imide solutions

The appropriate [Me−Py][NTf_2] isotopologues (*ca.* 5.0 g, 13 mmol) and protiated or deuteriated phenol (0.5 *eq.*, *ca.* 0.61 g) were accurately weighed under an inert, dry atmosphere in a glovebox and combined with heating at 60 °C producing, in each case, a free-flowing solution. The H/D isotopic substitutions in the four samples prepared are shown in Table 1. Mixtures were initially prepared at exactly 1:2 molar ratio phenol:ionic liquid (33 mol % phenol), however, after equilibration without agitation at 60 °C, a trace of a denser second phase was observed to separate from the bulk liquid. Integration of the signals from ^{1}H NMR spectroscopy of the bulk, homogeneous phase indicated that the liquid contained 34 mol % phenol. Cooling the samples to room temperature resulted in further phase separation, with crystallisation of excess

Table 1 Isotopic compositions of the four phenol solutions in *N*-methylpyridinium *bis*{(trifluoromethyl)-sulfonyl}imide measured.

	Methyl	Ring	Phenol
$[CD_3\text{-Py-}d_5][NTf_2]$ + phenol-d_6	D	D	D
$[CD_3\text{-Py-}d_5][NTf_2]$ + phenol-h_6	D	D	H
$[CH_3\text{-Py-}d_5][NTf_2]$ + phenol-d_6	H	D	D
$[CD_3\text{-Py-}h_5][NTf_2]$ + phenol-d_6	D	H	D

N-methylpyridinium *bis*{(trifluoromethyl)sulfonyl}imide from the liquid, producing a room temperature liquid with composition 38 mol % phenol determined from integration of ^{1}H NMR signals. ^{1}H-NMR and FTIR spectroscopic characterisation and data on the temperature dependence of viscosity and density of the 34 mol % phenol liquid are available as Supplementary Information, a detailed investigation of the phase characteristics as a function of composition has not been made at the current time. ^{1}H NMR (DMSO-d_6, 400 MHz): d = 4.36 (s, 6H), 6.75 (d, 1H), 6.78 (dt, 2H), 7.16 (t, 2H, *J* = 7.9 Hz), 8.12 (t, 4H, *J* = 6.82 Hz), 8.56 (t, 2H, *J* = 7.84 Hz), 8.98 (d, 4H, *J* = 5.9 Hz).

2.2 Neutron Scattering Data

Neutron scattering data were collected using the SANDALS instrument at the ISIS pulsed neutron and muon source, Rutherford Appleton Laboratory, UK. SANDALS has a wavelength range of 0.05–4.5 Å, with data being collected between $Q = 0.1$ to 50 Å^{-1}. Each sample was contained within null-scattering $Ti_{0.68}Zr_{0.32}$ flat-plate cells with internal dimensions $1 \times 35 \times 35$ mm with wall thickness of 1 mm. Throughout the data collection periods, the cell was maintained at 60 ± 0.5 °C using a Julabo recirculating heater.

Measurements were made on each of the empty sample holders, the empty spectrometer, and a 3.1 mm thick vanadium standard sample for the purposes of instrument calibration and data normalisation. After appropriate normalisation of the cell and window material, acceptable reproducibility could be seen for the sample cells. Data was collected from the four liquid solutions of phenol in *N*-methylpyridinium *bis*{(trifluoromethyl)sulfonyl}imide at 34 mol % phenol shown in Table 1.

Data was reduced using the Gudrun program [46], to produce a differential cross section for each sample. Experimental scattering levels and sample densities were consistent with the correct isotopic compositions of each samples. Calibration and background subtraction was performed for single atom scattering to enable an interference differential scattering for each composition. Neutron scattering data was then analysed with the Empirical Potential Structure Refinement (EPSR) [47, 48] approach which uses a reverse Monte Carlo calculation with Lennard-Jones potentials with atom-centred point charges to compare residuals from the simulation with experimental data in *Q*-space. Chemical and physical reliability is ensured during the modelling process as the data and basic information related to the structure and total atomic density of the molecules are compared.

The experimental total structure factor, F(Q), was extracted from the neutron diffraction data for each sample and this was then used to create and improve a three-dimensional model of the liquid structure consistent with the experimental data using EPSR. Simulations were equilibrated with 2000-3000 cycles before accumulating and averaging data. The EPSR refinement was initialised using an equilibrated Monte Carlo simulation of 200 ion pairs (200 *N*-methylpyridinium cations and 200 *bis*{(trifluoromethyl)sulfonyl}imide anions) and 100 phenol molecules in a cubic box of dimension 47.62 Å at 60 °C, representing an atomic density of 0.0676 atoms $Å^{-3}$ consistent with the experimentally determined molecular density of the protiated liquid (1.465 g cm^{-3}). These selective isotopologues provided four unique data sets, furthering confidence in the EPSR-derived structure. To describe the distributions of cation, anion and phenol in the liquid, partial radial distribution functions were calculated using the SHARM subroutine within the EPSR program using the cation, anion and phenol centres of mass as a positions of reference for orientation.

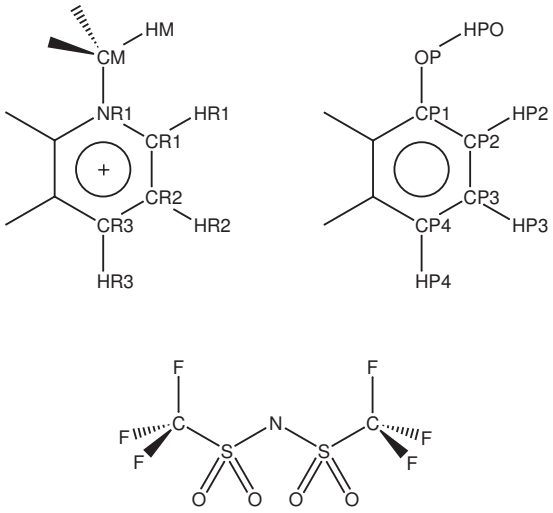

Fig. 1 Atom types of the [Me−Py]$^+$ cation (top left), phenol (top right) and [NTf_2]$^-$ anion used in the EPSR model.

Atom types were defined based on their unique positions in the molecular skeletons of phenol and the two ions, as shown in Figure 1. The full parameters of the reference potential used, derived from the OPLS-AA forcefield of Jorgensen *et al.* [49] for phenol, from Sambasivarao and Acevedo [50] for the pyridinium cation, and from Hardacre *et al.* [38] for the [NTf_2]$^-$ anion are given in Table 2. Table 3 summarises the interatomic distance and angular constraints used to define the basic molecular geometry of the cation, anion and phenol moieties within the model.

Table 2 Lennard-Jones (ε and σ) and charge (q) parameters used for the reference potential of the Empirical Potential Structure Refinement model

Atom type	ε (kJ mol^{-1})	σ (Å)	q (e)
Phenol			
CP2	0.8000	3.70	-0.1150
CP1	0.8000	3.70	0.1500
CP3	0.8000	3.70	-0.1150
HP2	0.2000	2.40	0.1150
OP	0.6500	3.10	-0.5850
CP4	0.8000	3.70	-0.1150
HP3	0.2000	2.40	0.1150
HPO	0.2000	2.40	0.4350
HP4	0.2000	2.40	0.1150
Anion			
N	0.7113	3.25	-0.6600
S	0.1046	3.55	0.1020
O	0.8786	2.96	-0.5300
C	0.2761	3.50	0.3500
F	0.2218	2.95	-0.1600
Cation			
CR1	0.2930	3.55	0.0397
NR1	0.7110	3.25	0.1824
CR2	0.2930	3.55	-0.2503
HR1	0.1260	2.42	0.1727
CM	0.2930	3.55	-0.3979
CR3	0.2930	3.55	0.1304
HR2	0.1260	2.42	0.2123
HM	0.1260	2.42	0.1916
HR3	0.1260	2.42	0.1615

3 Results and Discussion

The liquid structure of the phenol/ionic liquid solutions was analysed by EPSR simulation of the neutron diffraction data. Experimental neutron diffraction total differential cross scattering profiles, F(Q), and those calculated from EPSR simulation for the four experimental datasets are presented in Figure 2. Good agreement was observed for all isotopic substitutions between the experimental data and the EPSR derived model across the Q-range of interest which indicates consistency of the simulation model with the measured system.

From the EPSR model, centre of mass (COM) partial radial distribution functions calculated around cations, anions, and phenol were extracted and are shown in Figure 3. The radial distribution functions show cation-anion correlations clearly visible in the first coordination shell of both cation and anion and it is apparent that even with the addition of phenol at 50 mole % significant cation-anion structuring is present in the liquid. This is consistent with the concentric shell-like liquid structure [30, 51, 52] observed in ionic liquids and molten salts confirming that the intermolecular ion–ion correlations dominate the observed F(Q). This dominance of the Coulombic interactions on the scattering function has also been found in ionic liquids containing high concentrations of dissolved solutes, for example glucose in 1,3-dialkylimidazolium chloride and acetates [40], 1-methylnaphthalene in 1-methyl-4-

Table 3 Intramolecular bond distance (Å) and bond-angle (°) constraints used to define the basic structure of phenol, the *N*-methylpyridinium cation, and *bis*{(trifluoromethyl)sulfonyl}imide anion in the initial EPSR simulation model.

Bond Distance	(Å)	Bond Angle	(°)
Phenol			
CP2–CP1	1.40200	CP3–CP4–CP3	120.0
CP2–CP3	1.40200	CP3–CP4–HP4	120.0
CP2–HP2	1.09500	CP1–CP2–CP3	120.0
CP1–OP	0.94900	CP1–CP2–HP2	120.0
CP3–CP4	1.40200	CP3–CP2–HP2	120.0
CP3–HP3	1.09500	CP2–CP1–CP2	120.0
OP–HPO	0.94900	CP2–CP1–OP	120.0
CP4–HP4	1.09500	CP2–CP3–CP4	120.0
		CP2–CP3–HP3	120.0
		CP4–CP3–HP3	120.0
		CP1–OP–HPO	105.4
[Me−Py]$^+$			
CM–HM	1.10000	NR1–CR1–CR2	120.0
CR1–NR1	1.33700	NR1–CR1–HR1	120.0
CR1–CR2	1.37200	CR2–CR1–HR1	120.0
CR1–HR1	1.07200	CR1–NR1–CR1	120.0
NR1–CM	1.48100	CR1–NR1–CM	120.0
CR2–CR3	1.38700	CR1–CR2–CR3	120.0
CR2–HR2	1.07200	CR1–CR2–HR2	120.0
CR3–HR3	1.07400	CR3–CR2–HR2	120.0
		NR1–CM–HM	109.5
		HM–CM–HM	109.5
		CR2–CR3–CR2	120.0
		CR2–CR3–HR3	120.0
[NTf_2]$^-$			
C–S	1.81396	S–C–F	109.5
C–F	1.38158	F–C–F	109.5
S–N	1.77759	C–S–N	115.6
S–O	1.53640	C–S–O	112.6
		N–S–O	106.1
		O–S–O	102.8
		S–N–S	112.5

cyanopyridinium *bis*{(trifluoromethyl)sulfonyl}imide [38], and diethylamine in 1,3-dialkylimidazolium *bis*{(trifluoromethyl)sulfonyl}imide systems [39].

The cation first coordination shell contains both anions and phenol molecules. Both radial distribution functions (cation–anion and cation–phenol) show a broad maxima centred at approximately the same distance from the cation centre of mass (*ca.* 6 Å, and with no clear cation–cation correlation peak within this first shell co-ordination environment. The cation-phenol correlation is more tightly defined than the cation-anion, with the minima defining the first shell at *ca.* 7.5 Å compared

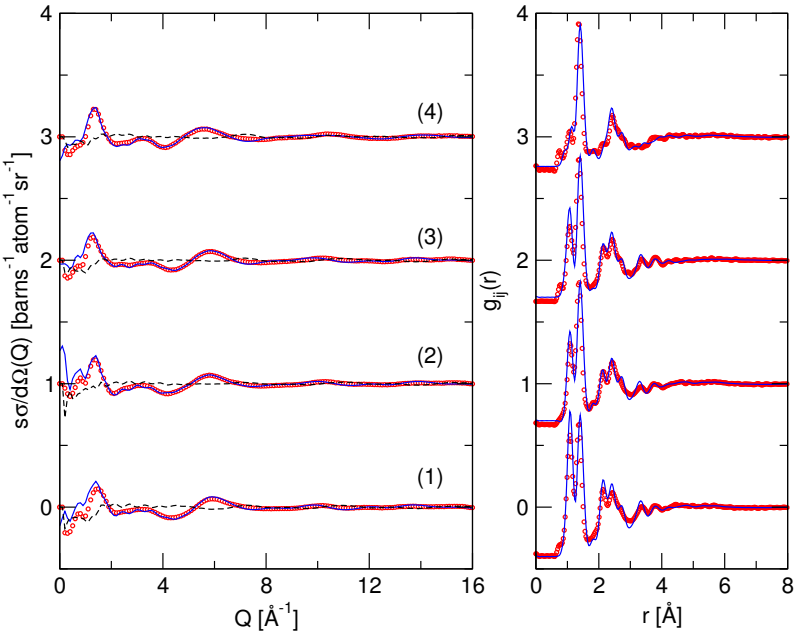

Fig. 2 Experimental (symbols) and EPSR modelled (solid line) total structure factors (left) and transformation to real space (right) for the four isotopically substituted liquid mixtures of [Me−Py][NTf_2] and phenol: (1) [CD_3-Py-d_5][NTf_2] + phenol-d_6; (2) [CD_3-Py-d_5][NTf_2] + phenol-h_6; (3) [CH_3-Py-d_5][NTf_2] + phenol-d_6; (4) [CD_3-Py-h_5][NTf_2] + phenol-d_6. Residual differences between the experimental and simulated data are shown by the dashed lines. The curves have been arbitrarily shifted.

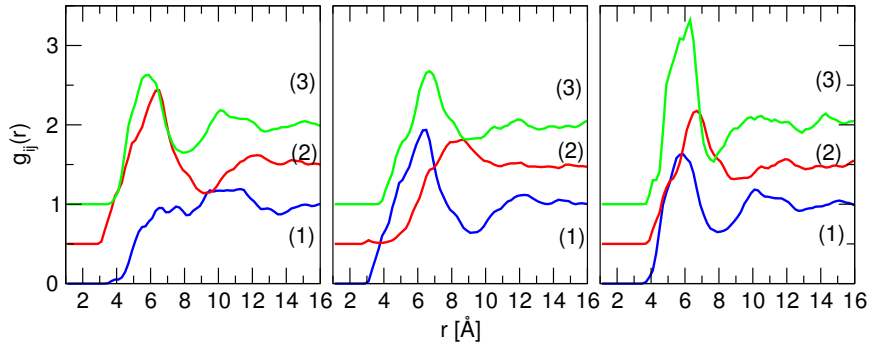

Fig. 3 Centre of mass radial distribution functions around the cation (left), anion (centre) and phenol (right) showing correlations with cations (1), anions (2) and phenol (3) as solid lines. The curves have been arbitrarily shifted.

to *ca.* 8.5 Å, however this may simply represent the larger volume occupied by the $[NTf_2]^-$ anion compared to phenol. Similarly, the anions show anion-cation and anion-phenol correlations in the first shell, although the maximum in the first peak in the anion-phenol radial distribution correlation is at a longer distance from the anion centre of mass *ca.* 7 Å than that of the anion-cation correlation.

These differences in the first shell environment is most clearly seen comparing the cation and anion correlations to phenol in figure 3 which show a closer approach of cations to the phenol in the first shell and a double-maxima in the phenol-anion correlation suggesting preferential and different interaction environments of phenol with the cation and anion. In this way, the behaviour of phenol dissolved in the ionic liquid is largely analogous to that of other aromatic solutes; benzene in [C_1mim][PF_6] [37] and 1-methylnaphthalene in [CN−MePy][NTf_2] [38]. However, unlike these non-polar aromatic solutes, a directional correlation between the acidic hydrogen-bond donating -OH group of phenol and the anions of the ionic liquid might be anticipated here. Such a correlation is not evident from the centre of mass radial distributions shown in Figure 3, however, if the specific site-site correlations are considered then preferential interactions of the phenol-OH group become evident with distinct correlations to anions through the charge bearing central SO_2−N−SO_2 region (HPO···O centred at 2.55 Å with a weaker HPO···N correlation as a consequence of steric crowding at the nitrogen centre by $-SO_2$ groups) and to hydroxyl groups of second phenols (HPO···HPO at 2.78 Å), as indicated by small peaks in the site-site correlation functions (Figure 4).

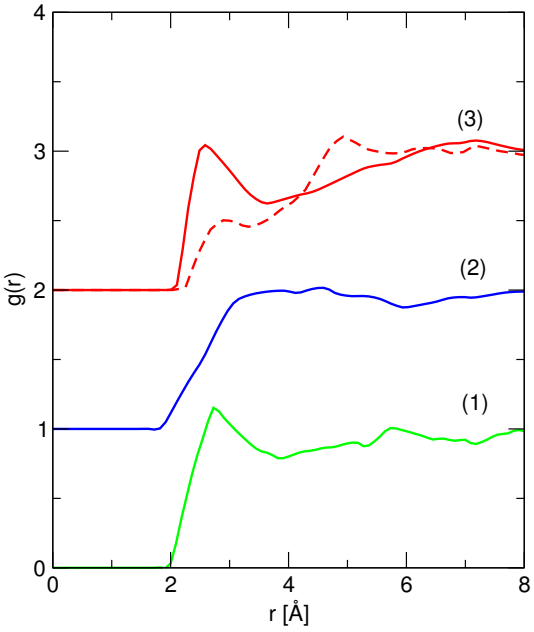

Fig. 4 Partial radial distribution functions derived from the EPSR models for the principle correlations of the phenol-OH group to (1) phenol HPO–HPO, (2) cation HPO–HM, and (3) anion HPO-O (solid) and HPO-N (dashed). The curves have been arbitrarily shifted.

The spatial probability distributions of *bis*{(trifluoromethyl)sulfonyl}imide anions and phenols around the *N*-methylpyridinium cation are shown in Figure 5. As previously observed for other species in ionic liquids, addition of phenol to the ionic

liquid led to little perturbation of the cation-anion spatial probability. Anions and phenols are both present within the first coordination shell of the pyridinium cations, as shown from the site-site radial distribution plots. From the spatial perspective, anions and phenols show a high probability for interaction with the cation over the plane of the aromatic ring and both display edge-on correlations within the plane of the cation ring. The anion correlation around the pyridinium cations in Figure 5 features four nodes in the plane of the ring, corresponding to interactions associated with the C(1/2) ring positions directed along the C-H bonds. In contrast, the phenol-cation correlation shows association in the ring plane perpendicular to the principle symmetry axis of the cation along the $N-CH_3$ bond. As such, anions and phenols occupy different space within the cation coordination sphere in the plane of the pyridinium ring, with mutual occupation of the space above and below the plane of the ring. Unusually, correlations of either anions or phenols with the pyridinium C(3)-H position are low.

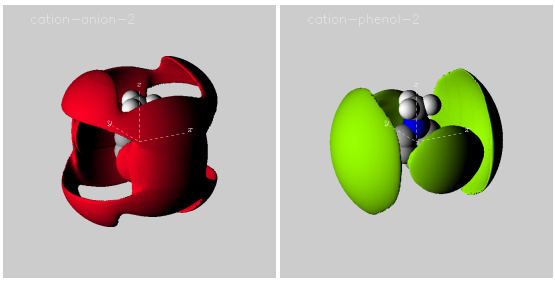

Fig. 5 Probability distributions of anions (left) and phenols (right) around a central methylpyridinium cation in the 1:2 phenol:[Me−Py][NTf_2] system from the EPSR model at 333 K. Surfaces are drawn to encompass the top 10% of ions within 8 Å (corresponding to the first minimum in the radial distribution functions).

The spatial probability distributions of methylpyridinium cations, *bis*{(trifluoromethyl)sulfonyl}imide anions and phenol around a central phenol molecule in the simulation are shown in Figure 6. The overall picture of the cation–aromatic and anion–aromatic probability distributions is similar to that previously reported for benzene and 1-methylnaphthalene in ionic liquids [37, 38] with significant differences in the positional distributions of cations and anions within the phenol solvation shell. The highest probability density for cations within the phenol first coordination shell is over the plane of the phenol ring, indicating a strong correlation of the cation with the electron-rich π-system of the phenol, and in the plane of the phenol ring perpendicular to the principle axis. The distribution of anions around central phenol within the first coordination shell is more diffuse with edge-interactions in the plane of the phenol ring. This is consistent with the interpretation of the centre-of-mass radial distributions which show the phenol-anion peak at a greater distance than the phenol-cation, corresponding to correlations with the edges rather than faces of the phenol ring. Surprisingly, the phenol-phenol probability distribution only reveals a small region of high correlation (corresponding to the peak at *ca.* 6 Å in the radial distribution

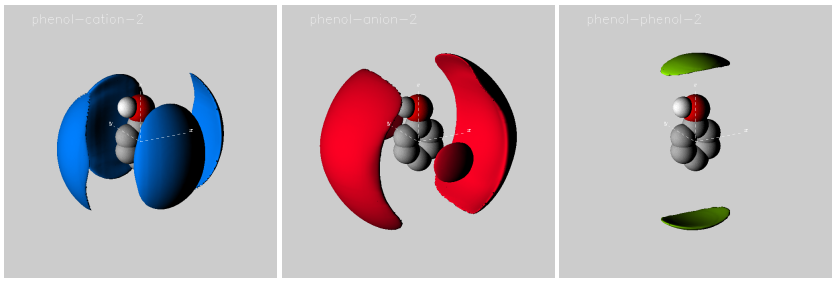

Fig. 6 Probability distributions of cations (left), anions (middle) and phenols (right) around a central phenol molecule in the 1:2 phenol:[Me−Py][NTf$_2$] system from the EPSR model at 333 K. Surfaces are drawn to encompass the top 10% of ions within 8 Å (corresponding to the first minimum in the phenol-cation and phenol-anion radial distribution functions).

function) along the C_2 axis of phenol, suggesting some residual structuring caused by the dipole moment of phenol, and reflecting the phenol OH···OH correlation shown in Figure 4. The spatial probability distributions reveal that, in the ionic liquid, phenol solvation occurs through facial interactions with the methylpyridinium cations and with an associated charge balancing distribution of anions surrounding the phenol ring edges.

It has been shown that increasing the alkyl-chain lengths in homogeneous series of ionic liquid cations can enhance phenol partitioning from water[17] in extraction studies. For an ionic liquid containing an aromatic cations (*e.g.* imidazolium, pyridinium *etc*), the cation–phenol association observed from the solution strucutre is clearly an important interaction mechanism and it is likely that extraction efficiency can be enhanced by selecting cations with greater aromatic character, as has been previously shown for the extraction of polyaromatic sulfur compounds from fuels [53]. If the potential to form phenol–anion interactions are considered as a mechanism to improve extraction, the phenol–anion correlation was observed to occur through directional short contacts from the phenol-OH groups to anions oxygens and through edge-on phenol ring to anion association. The presence of the O−H···H correlation support studies from Yang *et al.* [25] where ionic liquids containing anions with specific hydrogen-bond acceptor sites were identified as potentially good candidates to enhance interaction and extraction. The *bis*{(trifluoromethyl)sulfonyl}imide anion is a poor hydrogen-bond acceptor, and consequently does not strongly interact with phenol through hydrogen-bond donor–acceptor interactions (as exemlpified by the small HPO···O correlations in Figure 4. Increasing the ability of the anion to form hydrogen-bonds with -OH groups might lead to better interaction and extraction as predicted by Yang *et al.* [25], however, this would, in most cases also tend to reduce hydrophobicity which would have a detremental impact on the ability to form an ionic liquid-aqueous biphase necessary for solvent extraction. This is not a requirement for the DES approach to phenol extraction from oils [26, 27] and in this case, matching hydrogen-bond donor and acceptor potentials may be a good approach, rather than through cations modification to enhance lipophilicity or aromaticity.

4 Conclusions

The liquid structure and phenol coordination environment in a solution of phenol in *N*-methylpyridinium *bis*{(trifluoromethyl)sulfonyl}imide ionic liquid (1:2 ratio) has been determined using neutron diffraction. The phenol coordination environment contains cations and anions although the highest probability interactions are non-directional association of phenol with pyridinium cations over the faces of the phenol aromatic ring. Anion interactions appear to be primarily edge-on association with the phenolic C-H positions and are probably related to charge balancing to the cations. Additionally, a small site-site correlation of the phenol-OH group with both other phenols and the $[NTf_2]^-$ anion. These results suggest that enhanced solvent extraction of phenols by ionic liquids could be obtained by utilising cations with greater aromatic character, thus contributing to greater solvation of phenol through π–π interactions, or by introducing anions with greater hydrogen-bond acceptor character, thereby increasing the capacity for interaction with the phenol-OH group.

5 Acknowledgements

We acknowledge support from the Department of Education and Learning in Northern Ireland (DEL) for a PhD studentship to AHT, the Science and Technology Facilities Research Council (STFC) for beamtime under ISIS experiment (RB1410403), and Dr S. K. Callear for instrumentation support on SANDALS, ISIS.

References

1. Schobert, H., Song, C.: Chemicals and materials from coal in the 21st century. Fuel **81**, 15–32 (2002)
2. Deblonde, T., Cossu-Leguille, C., Hartemann, P.: Emerging pollutants in wastewater: A review of the literature. Int. J. Hyg. Environ. Health **214**, 442–448 (2011)
3. Yang, C., Qian, Y., Zhang, L., Feng, J.: Solvent extraction process development and on-site trial-plant for phenol removal from industrial coal-gasification wastewater. Chemical Engineering Journal **117**, 179–185 (2006)
4. Weber, M., Weber, M., Kleine-Boymann, M.: Phenol. In: Ullmann's Encyclopedia of Industrial Chemistry. Wiley-VCH Verlag GmbH & Co. KGaA (2000)
5. Weber, M., Weber, M.: Phenols. In: L. Pilato (ed.) Phenolic Resins: A Century of Progress, pp. 9–23. Springer-Verlag (2010)
6. Busca, G., Berardinelli, S., Resini, C., Arrighi, L.: Technologies for the removal of phenol from fluid streams: A short review of recent developments. J. Hazard. Mater. **160**, 265–288 (2008)
7. Greminger, D.C., Burns, G.P., Lynn, S., Hanson, D.N., King, C.J.: Solvent extraction of phenols from water. Ind. Eng. Chem. Proc. Des. Devel. **21**, 51–54 (1982)
8. Hallett, J.P., Welton, T.: Room-temperature ionic liquids: solvents for synthesis and catalysis. 2. Chem. Rev. **111**, 3508–3576 (2011)

9. Estager, J., Holbrey, J.D., Swadźba-Kwaśny, M.: Halometallate ionic liquids–revisited. Chem. Soc. Rev. **43**, 847–886 (2014)
10. Huddleston, J.G., Willauer, H.D., Swatloski, R.P., Visser, A.E., Rogers, R.D.: Room temperature ionic liquids as novel media for 'clean' liquid-liquid extraction. Chem. Commun. pp. 1765–1766 (1998)
11. Huddleston, J.G., Visser, A.E., Reichert, W.M., Willauer, H.D., Broker, G.A., Rogers, R.D.: Characterization and comparison of hydrophilic and hydrophobic room temperature ionic liquids incorporating the imidazolium cation. Green Chem. **3**, 156–164 (2001)
12. Bekou, E., Dionysiou, D.D., Qian, R.Y., Botsaris, G.D.: Extraction of chlorophenols from water using room temperature ionic liquids. In: R.D. Rogers, K.R. Seddon (eds.) Ionic Liquids As Green Solvents: Progress and Prospects, *ACS Symposium Series*, vol. 856, chap. 42, pp. 544–560. American Chemical Society (2003)
13. Vidal, S.T.M., Correia, M.J.N., Marques, M.M., Ismael, M.R., Reis, M.T.A.: Studies on the use of ionic liquids as potential extractants of phenolic compounds and metal ions. Sep. Sci. Technol. **39**, 2155–2169 (2004)
14. Inoue, G., Shimoyama, Y., Su, F., Takada, S., Iwai, Y., Arai, Y.: Measurement and correlation of partition coefficients for phenolic compounds in the 1-butyl-3-methylimidazolium hexafluorophosphate/water two-phase system. J. Chem. Eng. Data **52**, 98–101 (2007)
15. Shimoyama, Y., Ikeda, K., Su, F., Iwai, Y.: Effect of isomers on partition coefficients for phenolic compounds in the 1-butyl-3-methylimidazolium hexafluorophosphate plus water two-phase system. J. Chem. Eng. Data **55**, 3151–3154 (2010)
16. Katsuta, S., Nakamura, K.i., Kudo, Y., Takeda, Y., Kato, H.: Partition behavior of chlorophenols and nitrophenols between hydrophobic ionic liquids and water. J. Chem. Eng. Data **56**, 4083–4089 (2011)
17. Khachatryan, K.S., Smirnova, S.V., Torocheshnikova, I.I., Shvedene, N.V., Formanovsky, A.A., Pletnev, I.V.: Solvent extraction and extraction-voltammetric determination of phenols using room temperature ionic liquid. Anal. Bioanal. Chem. **381**, 464–470 (2005)
18. Ye, C., Zhou, O., Wang, X., Xiao, J.: Determination of phenols in environmental water samples by ionic liquid-based headspace liquid-phase microextraction coupled with high-performance liquid chromatography. J. Sep. Sci. **30**, 42–47 (2007)
19. Fan, Y.C., Chen, M.L., Shen-Tu, C., Zhu, Y.: A ionic liquid for dispersive liquid-liquid microextraction of phenols. J. Anal. Chem. **64**, 1017–1022 (2009)
20. Wang, Q., Qiu, H., Li, J., Liu, X., Jiang, S.: On-line coupling of ionic liquid-based single-drop microextraction with capillary electrophoresis for sensitive detection of phenols. J. Chromatogr. A **1217**, 5434–5439 (2010)
21. Lopez-Darias, J., Pino, V., Ayala, J.H., Afonso, A.M.: In-situ ionic liquid-dispersive liquid-liquid microextraction method to determine endocrine disrupting phenols in seawaters and industrial effluents. Microchim. Acta **174**, 213–222 (2011)

22. Nosrati, S., Jayakumar, N.S., Hashim, M.A.: Performance evaluation of supported ionic liquid membrane for removal of phenol. J. Hazard. Mater. **192**, 1283–1290 (2011)
23. Balasubramanian, A., Venkatesan, S.: Removal of phenolic compounds from aqueous solutions by emulsion liquid membrane containing ionic liquid [bmim][PF_6] in tributyl phosphate. Desalination **289**, 27–34 (2012)
24. Kumar, L., Banerjee, T., Mohanty, K.: Prediction of selective extraction of cresols from aqueous solutions by ionic liquids using theoretical approach. Sep. Sci. Technol. **46**, 2075–2087 (2011)
25. Yang, Q., Xing, H., Su, B., Bao, Z., Wang, J., Yang, Y., Ren, Q.: The essential role of hydrogen-bonding interaction in the extractive separation of phenolic compounds by ionic liquid. AIChE J. **59**, 1657–1667 (2013)
26. Pang, K., Hou, Y., Wu, W., Guo, W., Peng, W., Marsh, K.N.: Efficient separation of phenols from oils via forming deep eutectic solvents. Green Chem. **14**, 2398–2401 (2012)
27. Guo, W., Hou, Y., Wu, W., Ren, S., Tian, S., Marsh, K.N.: Separation of phenol from model oils with quaternary ammonium salts via forming deep eutectic solvents. Green Chem. **15**, 226–229 (2013)
28. Abbott, A.P., Capper, G., Davies, D.L., Rasheed, R.K., Tambyrajah, V.: Novel solvent properties of choline chloride/urea mixtures. Chem. Commun. pp. 70–71 (2003)
29. Guo, W., Hou, Y., Ren, S., Tian, S., Wu, W.: Formation of deep eutectic solvents by phenols and choline chloride and their physical properties. J. Chem. Eng. Data **58**, 866–872 (2013)
30. Hardacre, C., Holbrey, J.D., Nieuwenhuyzen, M., Youngs, T.G.A.: Structure and solvation in ionic liquids. Acc. Chem. Res. **40**, 1146–1155 (2007)
31. Hayes, R., Imberti, S., Warr, G.G., Atkin, R.: The nature of hydrogen bonding in protic ionic liquids. Angew. Chem. Int. Ed. **52**, 4623–4627 (2013)
32. Bowron, D.T., D'Agostino, C., Gladden, L.F., Hardacre, C., Holbrey, J.D., Lagunas, M.C., McGregor, J., Mantle, M.D., Mullan, C.L., Youngs, T.G.A.: Structure and dynamics of 1-ethyl-3-methylimidazolium acetate via molecular dynamics and neutron diffraction. J. Phys. Chem. B **114**, 7760–7768 (2010)
33. Hardacre, C., Holbrey, J.D., McMath, S.E.J., Bowron, D.T., Soper, A.K.: Structure of molten 1,3-dimethylimidazolium chloride using neutron diffraction. J. Chem. Phys. **118**, 273–278 (2003)
34. Jiang, H.J., FitzGerald, P.A., Dolan, A., Atkin, R., Warr, G.G.: Amphiphilic self-assembly of alkanols in protic ionic liquids. J. Phys. Chem. B **118**(33), 9983–9990 (2014). DOI 10.1021/jp504998t
35. Russina, O., Sferrazza, A., Caminiti, R., Triolo, A.: Amphiphile meets amphiphile: Beyond the polar-apolar dualism in ionic liquid/alcohol mixtures. J. Phys. Chem. Letts. **5**(10), 1738–1742 (2014)
36. Hayes, R., Imberti, S., Warr, G.G., Atkin, R.: How water dissolves in protic ionic liquids. Angew. Chem. Int. Ed. **51**, 7468–7471 (2012)
37. Deetlefs, M., Hardacre, C., Nieuwenhuyzen, M., Sheppard, O., Soper, A.K.: Structure of ionic liquid-benzene mixtures. J. Phys. Chem. B **109**, 1593–1598 (2005)

38. Hardacre, C., Holbrey, J.D., Mullan, C.L., Nieuwenhuyzen, M., Youngs, T.G.A., Bowron, D.T., Teat, S.J.: Solid and liquid charge-transfer complex formation between 1-methylnaphthalene and 1-alkyl-cyanopyridinium bis{(trifluoromethyl)sulfonyl}imide ionic liquids. Phys. Chem. Chem. Phys. **12**, 1842–1853 (2010)
39. Jacquemin, J., Bendova, M., Sedlakova, Z., Blesic, M., Holbrey, J.D., Mullan, C.L., Youngs, T.G.A., Pison, L., Wagner, Z., Aim, K., Gomes, M.F.C., Hardacre, C.: Phase behaviour, interactions, and structural studies of (amines plus ionic liquids) binary mixtures. ChemPhysChem **13**, 1825–1835 (2012)
40. Youngs, T.G.A., Holbrey, J.D., Mullan, C.L., Norman, S.E., Lagunas, M.C., D'Agostino, C., Mantle, M.D., Gladden, L.F., Bowron, D.T., Hardacre, C.: Neutron diffraction, nmr and molecular dynamics study of glucose dissolved in the ionic liquid 1-ethyl-3-methylimidazolium acetate. Chem. Sci. **2**, 1594–1605 (2011)
41. Youngs, T.G.A., Hardacre, C., Holbrey, J.D.: Glucose solvation by the ionic liquid 1,3-dimethylimidazolium chloride: A simulation study. J. Phys. Chem. B **111**, 13,765–13,774 (2007)
42. Cruz, H., Fanselow, M., Holbrey, J.D., Seddon, K.R.: Determining relative rates of cellulose dissolution in ionic liquids through in situ viscosity measurement. Chem. Commun. **48**, 5620–5622 (2012)
43. Swatloski, R.P., Spear, S.K., Holbrey, J.D., Rogers, R.D.: Dissolution of cellose with ionic liquids. J. Am. Chem. Soc. **124**, 4974–4975 (2002)
44. Holbrey, J.D., Reichert, W.M., Swatloski, R.P., Broker, G.A., Pitner, W.R., Seddon, K.R., Rogers, R.D.: Efficient, halide free synthesis of new, low cost ionic liquids: 1,3-dialkylimidazolium salts containing methyl- and ethyl-sulfate anions. Green Chem. **4**, 407–413 (2002)
45. Nakamura, Y., Maki, T., Wang, X., Ishihara, K., Yamamoto, H.: Iron(iii)-zirconium(iv) combined salt immobilized on n-(polystyrylbutyl)pyridinium triflylimide as a reusable catalyst for a dehydrative esterification reaction. Adv. Synth. Catal. **348**, 1505–1510 (2006)
46. Soper, A.K.: GudrunN and GudrunX: Programs for correcting raw neutron and x-ray diffraction data to differential scattering cross section. RAL Technical Report No. RAL-TR-2011-013, (2011)
47. Soper, A.K.: Empirical potential monte carlo simulation of fluid structure. Chem. Phys. **202**, 295–306 (1996)
48. Soper, A.: Tests of the empirical potential structure refinement method and a new method of application to neutron diffraction data on water. Mol. Phys. **99**, 1503–1516 (2001)
49. Jorgensen, W.L., Maxwell, D.S., TiradoRives, J.: Development and testing of the opls all-atom force field on conformational energetics and properties of organic liquids. J. Am. Chem. Soc. **118**, 11,225–11,236 (1996)
50. Sambasivarao, S.V., Acevedo, O.: Development of opls-aa force field parameters for 68 unique ionic liquids. J. Chem. Theory Comput. **5**, 1038–1050 (2009)
51. Padua, A.A.H., Gomes, M.F.C., Lopes, J.N.A.C.: Molecular solutes in ionic liquids: A structural, perspective. Acc. Chem. Res. **40**, 1087–1096 (2007)

52. Lynden-Bell, R.M., Del Popolo, M.G., Youngs, T.G.A., Kohanoff, J., Hanke, C.G., Harper, J.B., Pinilla, C.C.: Simulations of ionic liquids, solutions, and surfaces. Acc. Chem. Res. **40**, 1138–1145 (2007)
53. Holbrey, J.D., López-Martin, I., Rothenberg, G., Seddon, K.R., Silvero, G., Zheng, X.: Desulfurisation of oils using ionic liquids: selection of cationic and anionic components to enhance extraction efficiency. Green Chem. **10**, 87–92 (2008)